UDK 621.791:669.715
Original scientific article/Izvirni znanstveni članek

ISSN 1580-2949
MTAEC9, 48(4)491(2014)

EFFECT OF TUNNELING DEFECTS ON THE JOINT STRENGTH EFFICIENCY OBTAINED WITH FSW

VPLIV TUNELSKIH NAPAK NA UČINKOVITOST TRDNOSTI SPOJA, IZDELANEGA Z DRSNO MEŠALNIM VARJENJEM

Sebastian Balos, Leposava Sidjanin

Faculty of Technical Sciences, Department of Production Engineering, Trg Dositeja Obradovica 6, 21000 Novi Sad, Serbia
sebab@uns.ac.rs

Prejem rokopisa – received: 2013-08-14; sprejem za objavo – accepted for publication: 2013-09-13

In this paper, an attempt was made to study the effects of various types of tunneling defects in friction stir welding (FSW). Two types of welding tool were used, one with a threaded and the other with a polygonal pin. To enable the formation of tunneling defects, the shoulder-to-pin-volume ratio was larger than 1 for both tools, while the ratio of rotation speed to welding speed was optimized as well. Tunneling defects were tested on EN-AW 5052 H32 and H38 alloys, having the thicknesses of 3 mm and 8 mm. It was found that the threaded tool produced a single or double triangular, as well as crack-shaped tunnel. The polygonal tool produced a multiple triangular tunnel (the material flows toward the weld face) with a complex shape or a crack-type tunnel with a complex shape. The most unfavorable tunnel obtained with the polygonal tool was the crack-shaped one, resulting in the 62 % and 46 % joint yield and ultimate tensile-strength efficiency. The corresponding values for the threaded tool were 40 % and 36 %. The hardness efficiencies did not follow the trends of the proof and ultimate tensile strengths due to the prevention of the tunneling during indentation. Another effect on the hardness is the presence of microcracks that may influence the apparent decrease in the hardness in spite of the detected grain-refinement effect in the nugget. These effects influence the hardness distribution in the weld, shifting the maximum hardness value into the thermo-mechanical zone.

Keywords: friction stir welding, aluminium alloy, tunneling defect, joint strength efficiency

Članek predstavlja študij vpliva različnih vrst tunelskih napak pri drsno mešalnem varjenju (FSW). Uporabljeni sta bili dve vrsti varilnega orodja, eno z navoji in drugo s poligonalnim nastavkom. Da bi preprečili nastanek tunelske napake, je bilo razmerje med nosilcem in nastavkom večje od 1 pri obeh orodjih, medtem ko je bila optimirana tudi rotacija glede na hitrost varjenja. Tunelska napaka je bila preizkušena po EN-AW 5052 na zlitinah H32 in H38, debelih 3 mm in 8 mm. Ugotovljeno je bilo, da orodje z navoji povzroči enojni, dvojni trikotni tunel, kot tudi tunel v obliki razpoke. Poligonalno orodje povzroči več kompleksnih tunelov s trikotnim prerezom (material steče proti čelu zvara) ali kompleksnih vrst tunelov v obliki razpok. Najbolj nezaželen tunel, dobljen s poligonalnim orodjem, je bil v obliki razpoke, kar je povzročilo 62-odstotni in 46-odstotni izkoristek spoja oziroma učinkovitost natezne trdnosti. Ustrezne vrednosti pri orodju z navoji so bile 40 % in 36 %. Učinkovitost trdote ni sledila tem usmeritvam in končni natezni trdnosti zaradi izogibanja tunelom med merjenjem trdote. Nadaljnji vpliv na trdoto imajo mikrorazpoke, ki lahko povzročijo navidezno zmanjšanje trdote, kljub odkritemu zmanjšanju zrn v jedru zvara. Ti pojavi vplivajo na razporeditev trdote v zvaru in potiskajo vrednosti največje trdote v termomehansko območje.

Ključne besede: drsno mešalno varjenje, aluminijeva zlitina, tunelska napaka, učinkovitost trdnosti spoja

1 INTRODUCTION

Friction stir welding (FSW) is a solid-state metal-joining process that uses the third body (a specialized tool) to join two or more workpieces.[1] FSW has attracted considerable interest due to a number of advantages over arc-welding processes.[2] It has been shown that FSW may be suitable for joining materials that are difficult to join using conventional welding techniques such as 7XXX and 2XXX aluminium alloys.[3–7] Furthermore, Mg-alloys and dissimilar materials have been successfully welded with FSW.[8–13]

The microstructure and, therefore, the performance of the FSW welds strongly depend on the tool geometry as well as on the welding parameters such as the tool rotation and welding speeds. One of the main differences between the traditional arc-welding methods and FSW is the existence of the thermo-mechanically affected zone (TMAZ) near the heat-affected zone (HAZ) and the nugget.[14] The nugget takes the central place in the joint region. It is the most severely deformed region, often containing the equiaxed grains as the result of a dynamic recrystallization.[14] As the result of its position and the fact that the tool directly influences it, the nugget, together with the region above and under the nugget, may represent the zone where defects can occur.[15] One of the most critical types of the FSW defect is the tunneling. The tunneling defect occurs when the material flow around the tool pin is not adequate, resulting in an irregular weld filling.[16–18] In accordance with the results presented by Radisavljevic et al.[15], the ratio between the rotation and the welding speeds must be optimized. At the same time, an additional influencing factor might be the ratio between the pin volume and the reservoir in the tool shoulder (a concave shoulder volume) that should not exceed one in order to enable the material to pile up as a result of a pin indentation. In this work, an attempt was made to study the influence of the tunneling-defect shape and size on the mechanical properties of FSW joints, using two types of aluminium alloy.

2 EXPERIMENTAL PROCEDURE

Al-Mg plates in the half-hard condition (EN-AW 5052-H32) with a thickness of 3 mm and in the full-hard condition (EN-AW 5052-H38) with a thickness of 8 mm were used in this study. The chemical compositions of the plates, determined with an optical emission spectrometer ARL 3580, are given in **Table 1**. The mechanical properties of the workpiece materials, determined with a ZDM 5/91 tensile testing machine, are given in **Table 2**. The tensile properties were determined as the average of three specimens. The sample dimensions were 300 mm × 65 mm, forming a welded sample of 300 mm × 130 mm. The samples were tightly placed in a steel fixture with a backing plate into a 130 mm wide groove and secured with clamps (**Figure 1**). The fixture was fitted on an adapted Prvomajska UHG universal milling machine with a power of 5.2 kW. In this study, two different types of tool were used: plates 3 mm were welded with a polygonal-type tool, while plates 8 mm were welded with a threaded-type tool (**Figure 2**). Both tools were made of X38CrMoV5-1 (H11) hot-work tool steel, having a chemical composition as shown in **Table 3**. The chemical composition of the FSW tool material was measured with an optical emission spectrometer ARL 2460. The FSW tools were used in a heat-treated condition to 53 HRC. The tool concave-shoulder volume (reservoir) is larger than the pin volume in both tools used, stimulating the formation of a tunneling defect. For the polygonal-type tool, the shoulder-to-pin-volume ratio was 5.3 and for the threaded type it was 1.1, both being more than sufficient to store the piled up material as a result of the tool-pin indentation. Furthermore, the welding parameters were set to enable the formation of various types of the tunneling defect (**Table 4**). These parameters were set according to the results presented by Radisavljevic et

Figure 1: Test setup
Slika 1: Preizkusni sestav

Table 1: Chemical composition of EN-AW 5052 aluminium alloys (mass fractions, *w*/%)
Tabela 1: Kemijska sestava aluminijeve zlitine EN-AW 5052 (masni deleži, *w*/%)

	Cu	Mn	Mg	Si	Fe	Zn	Ti	Al
EN-AW 5052-H32	0.04	0.11	2.46	0.19	0.73	0.061	0.010	balance
EN-AW 5052-H38	0.03	0.29	2.33	0.19	0.29	0.011	0.022	balance

Table 2: Mechanical properties of EN-AW 5052-H32 and H38
Tabela 2: Mehanske lastnosti EN-AW 5052-H32 in H38

	Proof strength $R_{p0.2\ \%}$/MPa	Ultimate tensile strength R_m/MPa	Elongation %	Vickers hardness Number HV5
EN-AW 5052-H32	157 ± 3	214 ± 2	19 ± 1	67 ± 1
EN-AW 5052-H38	204 ± 7	245 ± 3	12 ± 1	90 ± 2

Table 3: Chemical composition of the X38CrMoV5-1 tool steel (*w*/%)
Tabela 3: Kemijska sestava orodnega jekla X38CrMoV5-1 (*w*/%)

C	Si	Mn	P	S	Cr	Mo	V	Fe
0.37	1.01	0.38	0.017	0.0005	4.85	1.23	0.32	balance

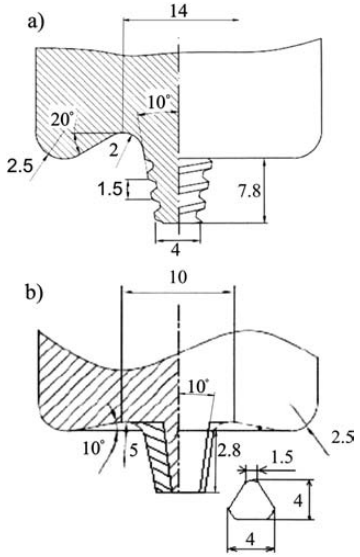

Figure 2: a) Threaded and b) polygonal tools
Slika 2: Orodje: a) z navoji, b) poligonalno orodje

Table 4: FSW parameters
Tabela 4: Parametri FSW

Sample	Rotation speed r/min	Welding speed mm/min	Rotation to welding speed r/mm	Tool rotation direction	Material flow direction
EN-AW 5052-H32; thickness 3 mm; polygonal-type tool					
1	1230	17	72.35	right	–
2	1230	12	102.50	right	–
3	1230	23	53.48	right	–
4	925	68	13.60	right	–
5	925	91	10.16	right	–
EN-AW 5052-H32; thickness 8 mm; threaded-type tool					
6	645	5	129.00	left	Up
7	645	5	129.00	right	Down
8	645	12	53.75	right	Down
9	645	49	13.16	right	Down

al.[15], where the welding speeds were in the range of 6.45–8.22 r/mm and the tool rotation direction was able to prevent the tunneling defect.

The mechanical properties of the FSW workpieces were determined with the tensile, root-bending and hardness tests as well as with a metallographic examination. The tensile and bending tests were carried out with a WPM ZDM 5/91 mechanical testing machine, according to EN 895 and EN 910 standards, respectively. The hardness was determined with a VEB HPO-250 Vickers testing machine, with a load 5 kg. The hardness measurements were done on the workpiece material (an average of five indentations) before and after the welding, to obtain the hardness profiles for the 1.5 mm distance between the indentations. The metallographic examinations were done with a light microscope Leitz Orthoplan, after a standard metallographic preparation. The metallographic preparation consisted of grinding (sandpaper, the grit of 220 to 2000), polishing (a diamond paste with (6, 3, 1 and ¼) μm particle sizes) and etching with Keller's reagent (2 mL HF, 3 mL HCl, 5 mL HNO_3, 190 mL H_2O).

3 RESULTS

3.1 Tensile properties

The tensile properties of FSW samples are presented in **Figure 3**. In Samples 1–5, it can be seen that the highest joint efficiencies are obtained with the higher tool rotation speed. Within this rotation speed, the highest joint proof-strength (PS) efficiency was obtained with a high end-welding speed, while the highest joint ultimate-tensile-strength (UTS) efficiency was obtained with the lowest welding speed. The lowest efficiencies were obtained with the lower tool rotation speed and the higher welding speed. A similar result was obtained with the EN-AW 5052-H38 alloy with a thickness of 8 mm, welded with a conceptually different tool, see Samples 6–9.

3.2 Root-bending test

In **Figure 4**, the root-bending-test results are shown. It can be seen that the highest angle of the first crack was obtained on Sample 1 (a base-material thickness 3 mm), while the lowest angle was obtained on Sample 6 (an base-material thickness 8 mm). On samples 1–8, the fracture did not occur up to 180°, while on Sample 9, the fracture occurred at 134°.

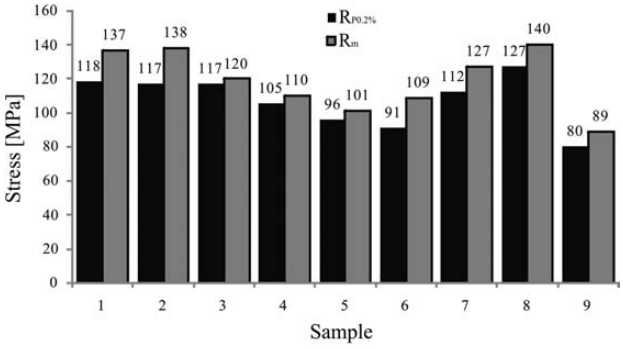

Figure 3: Joint proof and the ultimate tensile strengths of the tested samples
Slika 3: Preizkus spoja in končna natezna trdnost vzorcev

3.3 Hardness results

The Vickers-hardness (HV5) profiles of the representative samples are shown in **Figure 5**. In **Figures 5a** and **5b**, the hardness profiles for Samples 1 and 2 are shown, depicting the highest and the lowest tensile properties of the welded plates 3 mm. On the other hand, in **Figures 5c** and **5d**, the hardness profiles for Samples 8 and 9 are shown, depicting the highest and the lowest tensile pro-

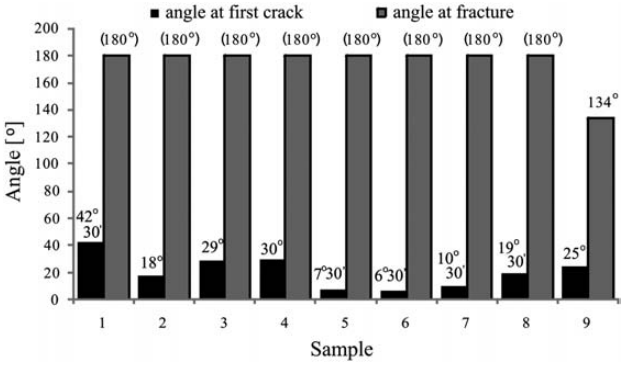

Figure 4: Results of the bending test. The values in parentheses represent the samples where no fracture occurred.
Slika 4: Rezultati upogibnega preizkusa. Vrednosti v oklepajih so za vzorce, kjer ni prišlo do zloma.

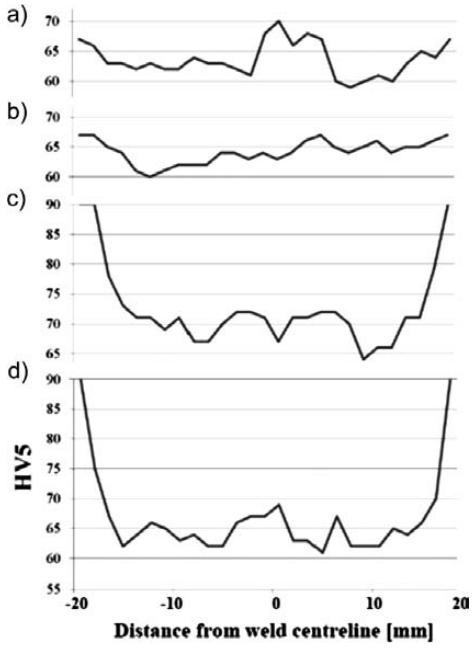

Figure 5: HV5 hardness profiles in relation to the distance from the centerline: a) sample 1, b) sample 5, c) sample 8, d) sample 9
Slika 5: Profil trdote HV5 v odvisnosti od razdalje od središča: a) vzorec 1, b) vzorec 5, c) vzorec 8, d) vzorec 9

perties of the welded plates 8 mm. In **Figures 5a**, **5c** and **5d** (Samples 1, 8 and 9) a common FSW hardness profile may be observed, while for Sample 5 (**Figure 5b**), an irregular profile was obtained. For Sample 1, the maximum hardness in the nugget (the weld centerline) is higher than that of the base material. For the other samples, all the hardnesses of the weld, in the thermo-mechanical zone and the heat-affected zone, are lower than that of the base material, indicating an insufficient grain refinement in certain FSW zones.

3.4 Macro and microstructure

The weld cross-sections of the specimens are shown in **Figure 6**, more exactly, in **Figures 6a** to **6e**, the weld cross-sections presented were obtained with the polygonal tool, while the ones from the second column, **Figures 6f** to **6i**, were obtained with the threaded tool. From these results it can be seen that with the polygonal tool, two types of the tunneling defect were achieved: a triangular (a closed tunneling defect) and a crack-shaped defect (an open tunneling defect). Tunnels might occur in a single (**Figure 6b**, Sample 2), double (**Figures 6a** and **6d**, Samples 1 and 4) or even triple configuration (**Figure 6c**, Sample 3). The crack-type tunneling defect obtained consisted of one longer and three smaller cracks (**Figure 6e**, Sample 5).

On the other hand, when the threaded-type tool was used, the tunneling defects with a more complex shape were obtained. The threaded-type tool with the material flow direction towards the tool (up) creates multiple tunnels, closely following the tool pin geometry. Such tunneling defects are spread across the whole weld cross-section. The material flow towards the weld root results in a complex-shaped tunneling defect in the weld center or at the bottom (**Figure 6f** to **6i**). Furthermore, a combination of the complex-shaped tunneling defect and the crack-shaped tunneling defect occurred on Sample 9 (**Figure 6i**).

The microstructures of the representative welded samples are shown in **Figure 7**. In **Figures 7a** to **7c**, the Sample 5 FSW zones are presented, while in **Figures 7d** to **7f**, the Sample 9 FSW zones are shown. It can be seen that the base-material microstructures, EN-AW 5052-H32 and H38 shown in **Figures 7a** and **7d**, correspond to the typical cold-rolled alloy, with a clearly visible deformed grain structure in the rolling direction. On the other hand, the heat-affected zones (HAZs) (**Figures 7b** and **7e**, both on the left of the micrograph) show coarsened recrystallized structures. In the thermo-mecha-

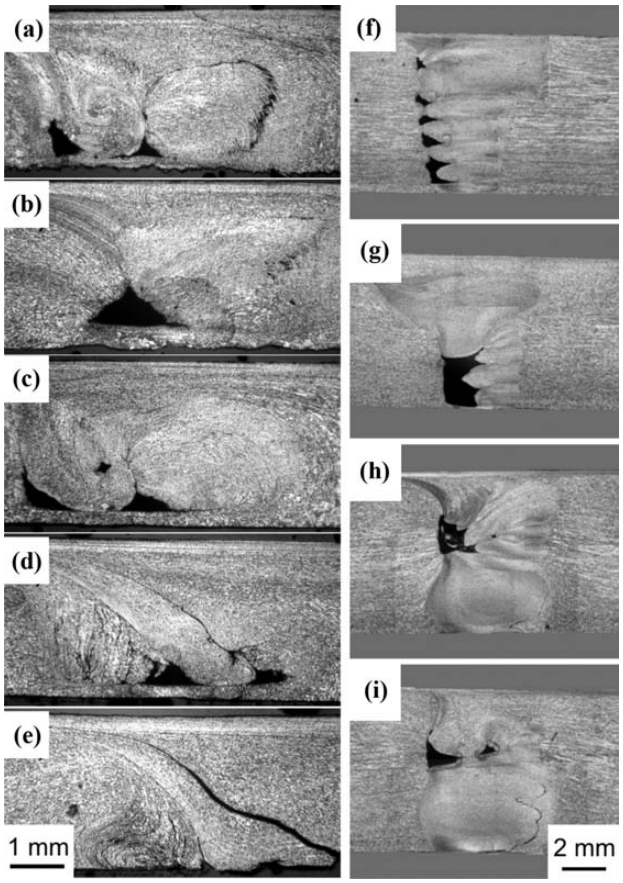

Figure 6: Weld cross-sections showing the tunnel profiles: a) sample 1, b) sample 2, c) sample 3, d) sample 4, e) sample 5, f) sample 6, g) sample 7, h) sample 8, i) sample 9

Slika 6: Prerezi zvara, ki prikazujejo profil tunela: a) vzorec 1, b) vzorec 2, c) vzorec 3, d) vzorec 4, e) vzorec 5, f) vzorec 6, g) vzorec 7, h) vzorec 8, i) vzorec 9

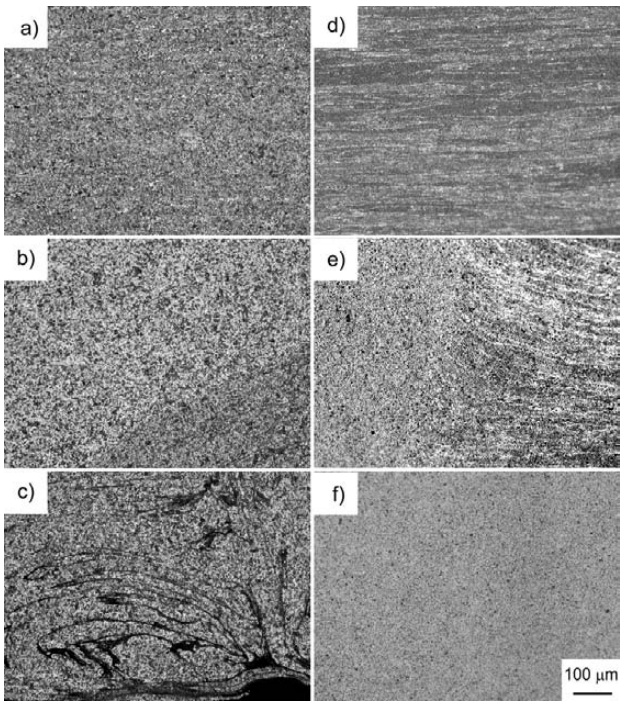

Figure 7: Microstructures of samples 5 and 9: a) sample 5: base material, b) sample 5: HAZ/TMAZ zone, c) sample 5: nugget, d) sample 9: base material, e) sample 9: HAZ/TMAZ zone, f) sample 9: nugget

Slika 7: Mikrostruktura vzorcev 5 in 9: a) vzorec 5: osnovni material, b) vzorec 5: področje HAZ/TMAZ, c) vzorec 5: jedro, d) vzorec 9: osnovni material, e) vzorec 9: področje HAZ/TMAZ, f) vzorec 9: jedro

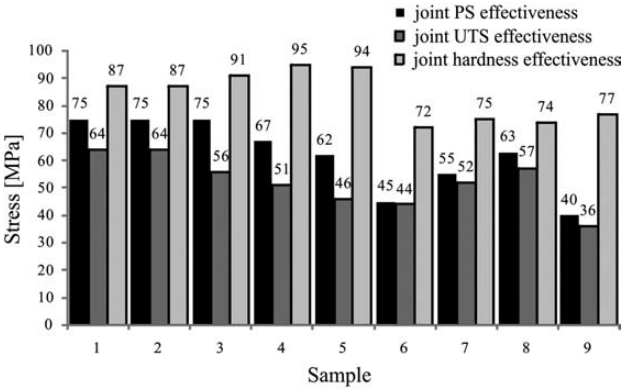

Figure 8: Joint PS, UTS and hardness effectiveness
Slika 8: Učinkovitost spoja PS, UTS natezne trdnosti in trdote

nical zones (TMAZs), shown in **Figures 7b** and **7e** (both to the right of the micrograph), finer microstructures are formed as a result of the local deformation. The main difference between **Figures 7c** and **7f**, where the nugget is depicted, is the occurrence of an intensive cracking, seen on Sample 5. In the Sample 9 nugget (**Figure 7f**), the microstructure is finer than that of the base material, HAZ and TMAZ.

4 DISCUSSION

4.1 Joint effectiveness to microstructure correlation

Joint PS, UTS and hardness effectiveness are given in **Figure 8**. According to the joint effectiveness shown in **Figure 8**, it can be seen that the joint UTS effectiveness is the lowest, followed by the joint PS effectiveness. The joint UTS effectiveness is lower than the values obtained by Radisavljevic et al. (by up to 80.1 %)[15], which is the result of the tunneling-type defect, as depicted in **Figure 4**. On the other hand, the joint hardness effectiveness matches the values obtained by Radisavljevic et al.[15] This is the result of the measuring method, according to which the indentations were made in the tunnel-free region of the weld, as well as the method of calculation. Namely, the maximum hardness was taken into account. However, although there is a correlation between the proof strength and the ultimate tensile strength, these two parameters cannot be correlated to the hardness effectiveness. Nevertheless, the hardness distributions may be correlated to the microstructures obtained, **Figures 6** and **7**, especially for the representative Samples 5 and 9. In Sample 5, the hardnesses of the nugget, TMAZ and HAZ are all similar, which is in contrast to the hardness values for Sample 9. There the nugget has a higher hardness than in the case of TMAZ and HAZ. As shown in **Figure 7**, the Sample 5 nugget contains a number of cracks that might have influenced the values that are similar to the ones for TMAZ and HAZ. On the other hand, in Sample 9, a crack-free nugget was obtained and, consecutively, higher hardnesses were measured than those for TMAZ and HAZ. Such a hardness distribution is the result of the grain refinement in the nugget. The nugget-hardness values are lower compared to the base material, which might be influenced by two factors: the grain refinement and the recrystallization.

4.2 Influence of the tunnel shape

The mechanical properties of the joints and their efficiencies clearly vary in accordance with the type of the FSW tool geometry. The two types of the FSW tool have different influences on the joint properties. It can be seen that the polygonal tool (Samples 1–5) produces joints with higher mechanical properties than the threaded tool (Samples 6–9) in spite of the higher shoulder-to-pin-volume ratio of 5.3 versus 1.1. The higher mechanical properties are influenced by the tunnel obtained. Namely, the polygonal tool produces triangular-shaped tunnels or crack-shaped tunnels that are the least optimal. The most optimum sample obtained with the polygonal-type tool is Sample 1 with a double tunnel, while the lowest mechanical properties were found for Sample 5 with a crack-shaped tunnel. Regarding the threaded-tool samples, the mechanical properties of Sample 8 are the highest, while the lowest mechanical properties were found for Sample 9. On Sample 9, a combination of a tunnel and a crack-shaped tunnel was found, which proved to have a more adverse effect on the mechanical properties compared to Sample 6, where multiple tunnels were found, closely following the tool-pin profile. The relatively high welding speeds applied in this study clearly did not contribute to the joint quality, regardless of the tool type.

5 CONCLUSIONS

According to the presented results, the following conclusions can be drawn:

- The UTS efficiency of the joints with the tunneling defect was lower by 25–82 % than that of the joints without the tunneling defect.
- The efficiency of the joint PS is higher than that of the ultimate tensile strength, while the hardness efficiency is higher than the joint PS efficiency.
- The tunnel profile is influenced by the pin geometry and pin direction determining the material flow direction.
- The polygonal-type tool produces a triangular tunnel shape, in single and multiple forms, as well as a crack-type tunneling defect.
- The threaded-type tool produces a triangular and complex-shaped tunnel, depending on the material flow direction. If the material flows towards the weld root a complex-shaped tunnel is formed with superior mechanical properties. The only exception is the combination of a complex-shaped and crack-type tunnel. In the case of an upward material flow,

multiple triangular tunneling defects are formed that are very unfavorable with respect to mechanical properties.
- The lowest mechanical properties both in terms of the tensile strength and bending were obtained with the tunneling defects associated with cracks.
- The highest joint efficiency was obtained with the polygonal-pin profile.
- The pin-to-concave-shoulder-volume ratio greatly influences the occurrence of the tunneling defect.

Aknowledgements

The authors are grateful to Mr. Michael A. Maier for his technical assistance.

6 REFERENCES

[1] W. M. Thomas, E. D. Nicholas, J. C. Needham, M. G. Murch, P. Templesmith, C. J. Dawes, International Patent Application No. PCT/GB92/02203, GB Patent Application No. 9125978.8 (Dec. 1991) and U.S. patent No. 5, 460, 317, (Oct. 1995)

[2] H. Khodaverdizadeh, A. Mahmoudi, A. Heidarzadeh, E. Nazari, Materials and design, 35 (**2012**), 330

[3] G. İpekoglu, B. G. Kiral, S. Erim, G. Çam, Mater. Tehnol., 46 (**2012**) 6, 627–632

[4] L. Fratini, G. Buqa, D. Palmeri, J. Hua, R. Shivpuri, Science and Technology of Welding and Joining, 11 (**2006**), 412

[5] R. S. Mishra, Z. Y. Ma, Materials science and engineering A, 50 (**2005**) 1/2, 1

[6] P. L. Threadgill, A. J. Leonard, H. R. Shercliff, P. J. Withers, International materials review, 54 (**2009**) 2, 49

[7] L. Magnusson, L. Kallman, Mechanical Properties of Friction Stir Welds in Thin Sheet of Aluminium 2024, 6013 and 7475, Proc. of the 2nd International Symposium on Friction Stir Welding, Gothenburg, Sweden, 2000, 26–28

[8] N. Afrin, D. L. Chen, X. Cao, M. Jahazi, Materials science and engineering A, 472 (**2008**), 179

[9] G. M. Xie, Z. Y. Ma, L. Geng, Materials science and engineering A, 486 (**2008**), 49

[10] S. M. Chowdhury, D. L. Chen, S. D. Bhole, X. Cao, Materials science and engineering A, 527 (**2010**), 6064

[11] T. Debroy, H. K. D. H. Bhadeshia, Science and Technology of Welding & Joining, 15 (**2010**) 4, 266

[12] O. Frigaard, A Process Model for FSW of Age Hardening Aluminium Alloys, Ph.D. Thesis, Norwegian University of Science and Technology, 1999

[13] J. Quyang, R. Kovacevic, Journal of Materials Engineering and Performance, 11 (**2002**), 51

[14] K. V. Jata, S. L. Semiatin, Continuous Dynamic Recrystallization During FSW of High Strength Aluminium Alloys, Scripta Materialia, 43 (**2000**), 743

[15] I. Radisavljevic, A. Zivkovic, N. Radovic, Avoidance of tunnel type defects in FSW welded Al 5052-H32 plates, Welding & Welded Structures, 1 (**2012**) 1, 5–11

[16] R. Nandan, T. Debroy, H. Bhadeshia, Recent Advances in Friction Stir Welding: Process, Weldment structure and Properties, Progress in Materials Science, 53 (**2008**), 980

[17] H. Bhadeshia, Joining of Commercial Aluminium Alloys, Proc. of the International Conference on Aluminium, Bangalore, India, 2003, 195–204

[18] K. Kumar, S. V. Kailas, The Role of Friction Stir Welding Tool on Material Flow and Weld Formation, Material Science and Engineering, 485 (**2008**), 367